Mechanism of interaction of hydrocalumites (Ca/Al-LDH) with methyl orange and acidic scarlet GR

Ping Zhang [a,b,c], Guangren Qian [*b], Huisheng Shi [a], Jing Yang [c], Ray L. Frost [*c]

[a] *Key Laboratory of Advanced Civil Engineering Materials (Tongji University), Ministry of Education, Shanghai 200092, PR China;*

[b] *School of Environmental and Chemical Engineering, Shanghai University, Shanghai 200072, PR China.*

[c] *Chemistry Discipline, Faculty of Science and Technology, Queensland University of Technology, GPO Box 2434, Brisbane Queensland 4001, Australia.*

Corresponding Authors:

Ray L. Frost: Tel: +61-7-3138 2407;
Fax: +61-7-3138 2407
Email: r.frost@qut.edu.au

Prof. Guangren Qian: Tel: +86-21-56338094;
Fax: +86-21-56333052
Email: grqian@shu.edu.cn

Graphical Content for

Mechanism of interaction of hydrocalumites (Ca/Al-LDH) with methyl orange and acidic scarlet GR

Ping Zhang [a,b,c], Guangren Qian [*b], Huisheng Shi [a], Jing Yang [c], Ray L. Frost [*c]

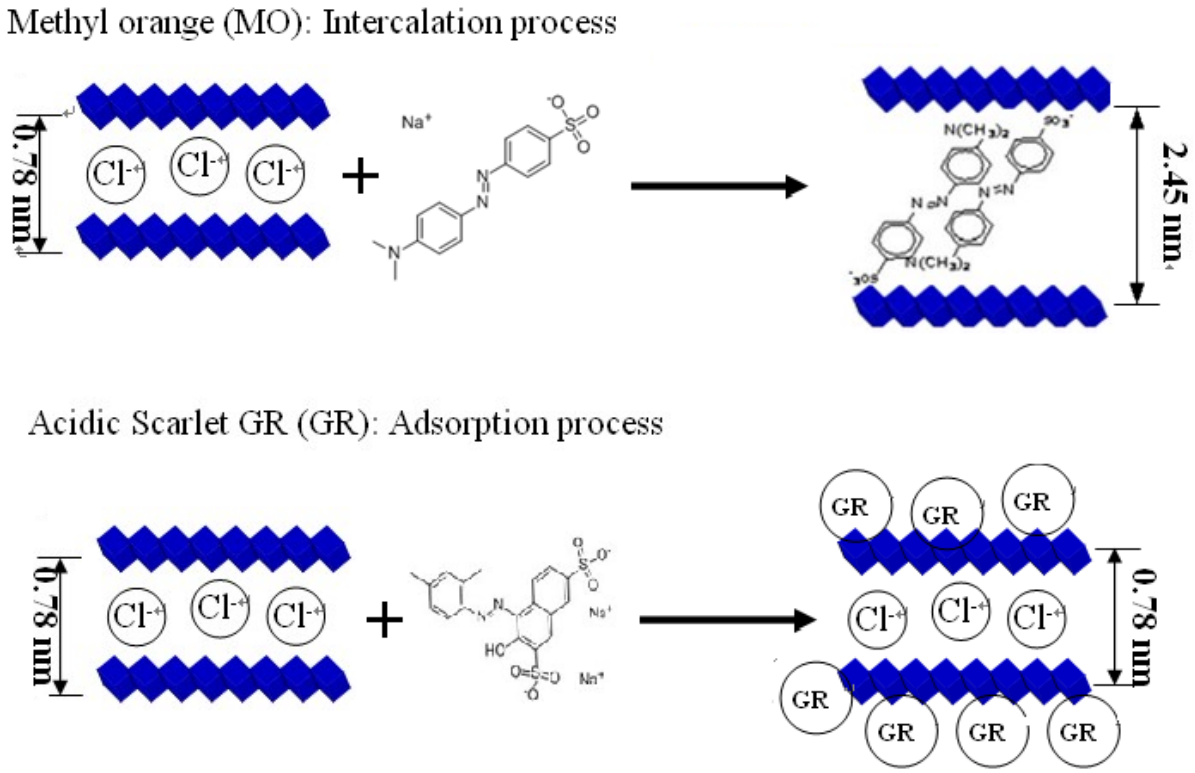

Methyl orange and acidic scarlet GR have different mechanisms of interaction with Ca/Al-LDH-Cl. Methyl orange is through intercalation into the Ca/Al-LDH-Cl layers, while acidic scarlet GR is simply adsorbed onto the Ca/Al-LDH-Cl surfaces.

Abstract

The development of new materials for water purification is of universal importance. Among these types of materials are layered double hydroxides (LDHs). Non-ionic materials pose a significant problem as pollutants. The interaction of methyl orange (MO) and acidic scarlet GR (GR) adsorption on hydrocalumite (Ca/Al-LDH-Cl) were studied by X-ray diffraction (XRD), infrared spectroscopy (MIR), scanning electron microscope (SEM) and near-infrared spectroscopy (NIR). The XRD results revealed that the basal spacing of Ca/Al-LDH-MO was expanded to 2.45 nm, and the MO molecules were intercalated with a inter-penetrating bilayer model in the gallery of LDH, with 49^{o} tilting angle. Yet Ca/Al-LDH-GR was kept the same d-value as Ca/Al-LDH-Cl. The NIR spectrum for Ca/Al-LDH-MO showed a prominent band around 5994 cm^{-1}, assigned to the combination result of the N-H stretching vibrations, which was considered as a mark to assess MO^{-} ion intercalation into Ca/Al-LDH-Cl interlayers. From SEM images, the particle morphology of Ca/Al-LDH-MO mainly changed to irregular platelets, with a “honey-comb” like structure. Yet the Ca/Al-LDH-GR maintained regular hexagons platelets, which was similar to that of Ca/Al-LDH-Cl. All results indicated that MO^{-} ion was intercalated into Ca/Al-LDH-Cl interlayers, and acidic scarlet GR was only adsorped upon Ca/Al-LDH-Cl surfaces.

Keywords: Hydrocalumites; methyl orange (MO); acidic scarlet GR (GR);

52 intercalation; adsorption; near-infrared spectroscopy (NIR)

1. Introduction

LDHs, also known as anionic clays, have positively charged metal oxides/hydroxides sheets compensated by anions in the interlayer. Generally it is represented by the general formula $\{M^{2+}_{1-X}M^{3+}_{X}(OH)_2\}A_{x/n}\cdot yH_2O$, where M^{2+} and M^{3+} are metal cations, $x=M^{3+}/(M^{2+}+M^{3+})$ and A^{n-} denotes the interlayer anions [1].

Because of the flexibility in composition and the exchangability of interlayer anions, LDHs possess a wide variety of properties. These materials have applications in various fields, such as catalysis, adsorbents, ion exchanges, pharmaceutics, purification, etc. [2-6]. Recently there is a growing interest focusing on using these materials for synthesis of organoclay modified organic materials [7, 8], whose hydrophilic surfaces could be changed to hydrophobic ones. The resulting products can be used to remove non-ionic organic compounds from the environment [6, 9].

In general, hydrocalumite ($[Ca_2(Al,Fe)(OH)_6]^+X^-\cdot mH_2O$) is expressed as AFm, with a similar structure to that of LDHs, where X^- is an anion, such as OH^-, Cl^-, SO_4^{2-}, and CO_3^{2-}. Hydrocalcumite can easily form in the hydrated cement paste, and thus can be cheaply prepared [10, 11]. Particularly, $Ca_2Al(OH)_6Cl(H_2O)_2$ (Ca/Al-LDH-Cl) is a major hydration product, which is found in concrete submerged in seawater and subjected

74 to Cl^- corrosion [12]. Cl^- has less affinity for hydrocalumite, thus
75 Ca/Al-LDH-Cl and be easily exchanged to form other types of
76 Ca/Al-LDH by using Na-dodecylsulfate (SDS) , PO_4^{3-} and oxyanions
77 possibly [13-15].

78 Methyl orange (MO) and acidic scarlet GR (GR) are common dyes and
79 widely used in industry [16, 17]. They are not only undesirable pollutants,
80 but coloration of water by the dyes may interfere with light penetration
81 affecting aquatic ecosystems [18]. Nowadays the conventional methods
82 for dye materials removal from contaminated water involved processes,
83 such as physical, chemical, biological methods, electrochemical oxidation
84 and adsorption methods [19-24]. Among the proposed treatment methods,
85 adsorption technologies is regarded as one of the competitive methods
86 due to potential low-cost, high efficiency, simplicity of design/operation
87 [25], and adsorption materials contain activated carbon, activated rice
88 husk, bottom ash and so on [21, 24, 26-28], yet after adsorbing dye
89 pollutions, their by-products were difficult to recycle. Recently, Some
90 reports mentioned that methyl orange or acidic scarlet GR could be
91 removed effectively by Mg/Al-LDH [29], Zn/Al-LDH [30] through
92 intercalation reaction. Moreover, LDHs can be calcined to the mixed
93 oxides (LDOs) [31], and LDOs have been examined to adsorb methyl
94 orange and orange II from water again [17, 32]. Base on above statements,
95 we can proposal that LDHs are able to be exploited as valuable and

recyclable adsorption materials to removal dye material.

In the present study, Ca/Al-LDH-Cl reacts with methyl orange and acidic scarlet GR, and the subsequent effects on the structure and the morphology by X-ray diffraction (XRD), mid-infrared spectroscopy (MIR), scanning electron microscope (SEM) and near-infrared spectroscopy (NIR) were studied. Another objective of this study is to define the removal mechanism for methyl orange and acidic scarlet GR with Ca/Al-LDH-Cl. It is worth mentioning that near-infrared (NIR) and mid-infrared (MIR) spectroscopy were used to investigate changes for the structure of layered materials intercalated with organic molecules. One of fast and non-destructive analytical method [33, 34], NIR and MIR spectra can show the appearance of new bands as comprehensive evidence of the intercalation process. [35-37]. There have been few reports of using NIR spectroscopy in the Ca/Al-LDH-Cl intercalation.

2. Materials and methods

2.1 Materials

Aluminum hydroxide ($Al(OH)_3$, AR grade), calcium oxide (CaO, AR grade), calcium chloride ($CaCl_2 \cdot 6H_2O$, GA grade), methyl orange ($C_{14}H_{14}N_3NaO_3S$, MW: 327.34, abbreviated as MO), and acidic scarlet GR ($C_{18}H_{14}N_2Na_2O_7S_2$, MW: 556.49, abbreviated as GR here) were purchased

116 from Shanghai Kechuang Co. Ltd. All chemicals were used as received.

117 ***2.2 Materials synthesis***

118 ***2.2.1. Preparation of precursor material***

119 The Ca/Al-LDH-Cl was prepared by the following method [13]: 5.94 g
120 powdered $3CaO \cdot Al_2O_3$ (synthesized by solid reaction at 1350 ^oC) was
121 slowly added into a solution containing 4.82 g $CaCl_2 \cdot 6H_2O$ and stirred for
122 18 h under N_2 gas atmosphere at 55 ^oC. Then, the precipitate was collected
123 by filtration after aging 24 h at the same temperature, and then washed
124 with deionized water and dried at 100 ^oC in the oven, ground and stored in
125 a glass container.

126 ***2.2.2. Preparation of two modified Ca/Al-LDHs with MO and GR***

127 0.1 g Ca/Al-LDH-Cl was added to methyl orange or acidic scarlet GR
128 aqueous solutions (20 ml) with concentrations of 0.2 M. The mixture was
129 centrifuged after stirring 24 h at 25 ^oC . The precipitate was dried at 70 ^oC
130 for 24 h in the oven, then ground, passed through a 100-mesh sieve. Finally,
131 the two intercalation samples were stored into a plastic bottle for
132 characterization.

133 ***2.3. Characterization of materials***

134 ***2.3.1. X-ray diffraction***

The X-ray diffraction (XRD) data were collected at room temperature in a D/max RBX diffractometer with Cu Kα (40 kV, 100 mA) radiation. Ca/Al-LDH was scanned at a rate of 6° per minute in the 2θ range of 5°-65°. For the samples modified by methyl orange and acidic scarlet GR, the XRD data were collected in two sections: the first section was scanned from 1° to 5° using silts 1/6 (divergence), 1/6 (anti-scattering) and 0.15 (receiving) at a rate of 0.5° per minute and the second section from 5° to 65° using silts 1/6 (divergence), 1/6 (anti-scattering) and 0.30 (receiving) at a rate of 6° per minute.

2. Mid-infrared spectroscopy

Mid-infrared spectra were obtained in reflectance mode using a Nicolet Nexus 870 Fourier transform infrared spectroscopy (FTIR) spectrometer with a smart endurance single bounce diamond ATR cell. Spectra over the 4000–600 cm^{-1} range were obtained by the co-addition of 64 scans with a resolution of 4 cm^{-1} and a mirror velocity of 0.6329 cm/s. Spectra were co-added to improve the signal to noise ratio.

3. Near-infrared spectroscopy

Near-infrared spectra were collected in reflectance mode using a Nicolet Nexus FT-IR spectrometer with a Nicolet Near-IR Fibreport accessory (Nicolet Nexus, Madison, Wisconsin, USA). A white light source was used,

155 with a quartz beam splitter and TEC NIR InGaAs detector. Spectra were
156 obtained from 12000 to 4000 cm^{-1} (909-2500 nm) by the co-addition of 64
157 scans at a resolution of 8 cm^{-1}. A mirror velocity of 1.2659 m/s was used.

158 The spectral manipulations of baseline adjustment, smoothing and
159 normalization were performed using the Spectracalc software package
160 GRAMS (Galactic Industries Corporation, NH, USA). Band component
161 analysis was carried out using Peakfit software (Jandel Scientific, Postfach
162 4107, D-40688 Erkrath, Germany). Lorentz-Gauss cross product functions
163 were used throughout and peakfit analysis undertaken until squared
164 correlation coefficients with r^2 >0.998 were obtained.

165 ***4. Scanning electron microscope (SEM)***

166 The morphology of samples was observed by using a scanning electron
167 microscope (SEM), Hitachi S-4800. Samples were coated with a
168 gold/palladium film and the SEM images were obtained using a secondary
169 electron detector.

170 **3. Results and discussion**

171 ***3.1. X-ray diffraction***

172 **Fig.1 XRD patterns of samples of Ca/Al-LDH-Cl, Ca/Al-LDH-MO**
173 **and Ca/Al-LDH-GR scanned from 5°-65° (a) and 1°-15° (b)**

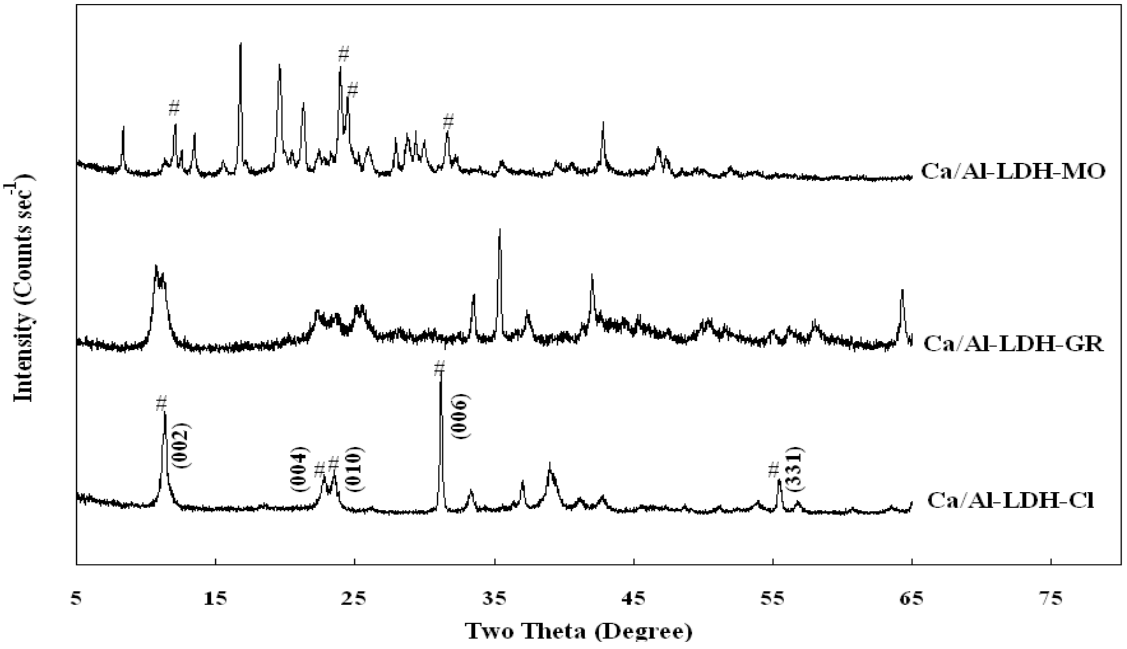

174

175 (a)

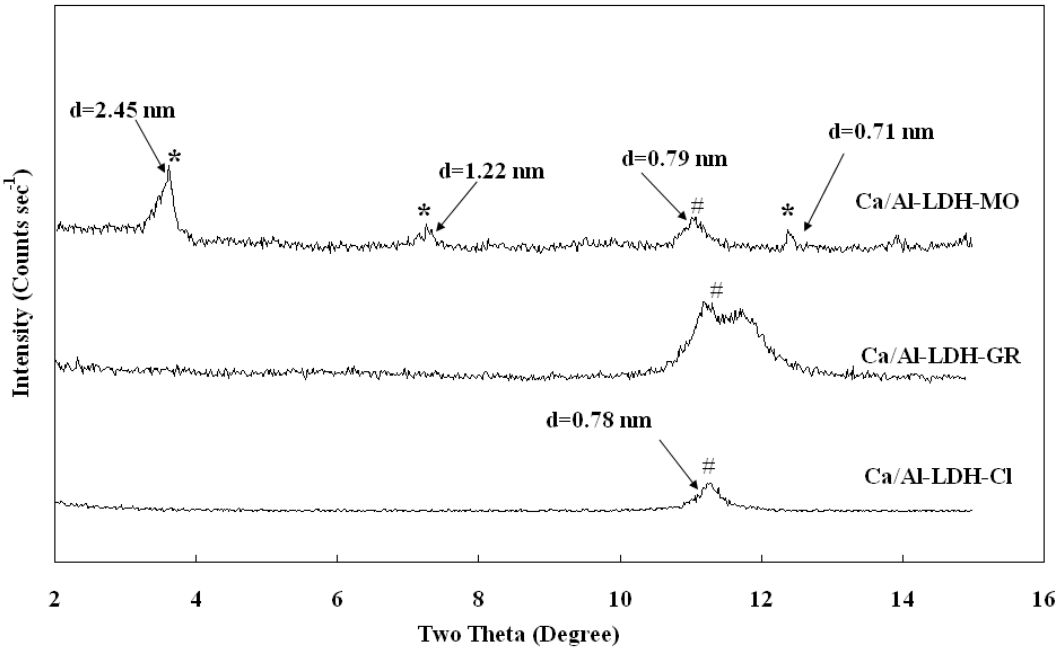

176

177 (b)

178 The XRD patterns of Ca/Al-LDH-Cl and two modified LDHs by

179 methyl orange and acidic scarlet GR were shown in Fig.1. The XRD

pattern of the as-synthesized Ca/Al-LDH-Cl was in excellent agreement with that recorded on PDF78-1219 in the database of the International Center for Diffraction Data, with a nominal chemical formula of $Ca_4Al_2(OH)_{12}Cl_2(H_2O)_4$. Ca/Al-LDH-Cl displayed peaks corresponding to (002), (004), (010), (006) and (110) crystal planes (Fig.1), indicating relatively well-formed crystalline layered structure, with the basal spacing $d_{(002)}$ was 0.78 nm. After MO was interacted with Ca/Al-LDH-Cl, the new set of basal diffraction reflections from Ca/Al-LDH-MO were observed at 3.6^o, 7.26^o and 12.38^o (2θ) in Fig.1 (marked with *), and their corresponding distances of spacing appeared multiple relationship, respectively, which were similar to those reported by the authors [38, 39]. It was indicated that Ca/Al-LDH-MO kept a good double layer structure, and an intercalation of MO^- ion into the LDH interlayer space, with the d-value 2.45 nm. Yet it is obvious that some peaks of Ca/Al-LDH-Cl were still existed in XRD pattern of Ca/Al-LDH-MO, suggesting that intercalation did not finish completely between MO^- ion and Cl^- in the LDH interlayers. Usually, the conformation of intercalated anions in the interlayer of LDHs can be deduced from the d-spacing value of the resultant materials. In theory, the dimension of the long axis of the MO molecule is 1.31 nm [16], and the thickness of one LDHs sheet is about 0.48 nm, so it was easily calculated that a basal spacing of 1.79 nm and 3.10 nm would be observed for monolayer and bilayer models with

perpendicular orientation of the MO in the interlayer, respectively. In fact, the d-value of Ca/Al-LDH-MO was 2.45 nm. Therefore, we could infer that the MO molecules may be intercalated into the gallery of LDHs with a inter-penetrating bilayer model, and its tilting angle was calculated about 49^{o}.

In comparison, the XRD patterns of Ca/Al-LDH-GR were similar to that Ca/Al-LDH-Cl. No new basal diffraction reflections were observed; some peaks becoming broader and the (110) peak disappeared, indicating the crystalline of LDH became worse. In fact, based upon our studies, it was concluded that acidic scarlet GR was not intercalated into LDH interlayers.

3.2. Mid-infrared spectroscopy

3.2.1. The 1800-600 cm^{-1} spectral region

Fig.2 The 1800 - 600 cm^{-1} region of IR spectra of samples of Ca/Al-LDH-Cl , Ca/Al-LDH-MO and Ca/Al-LDH-GR

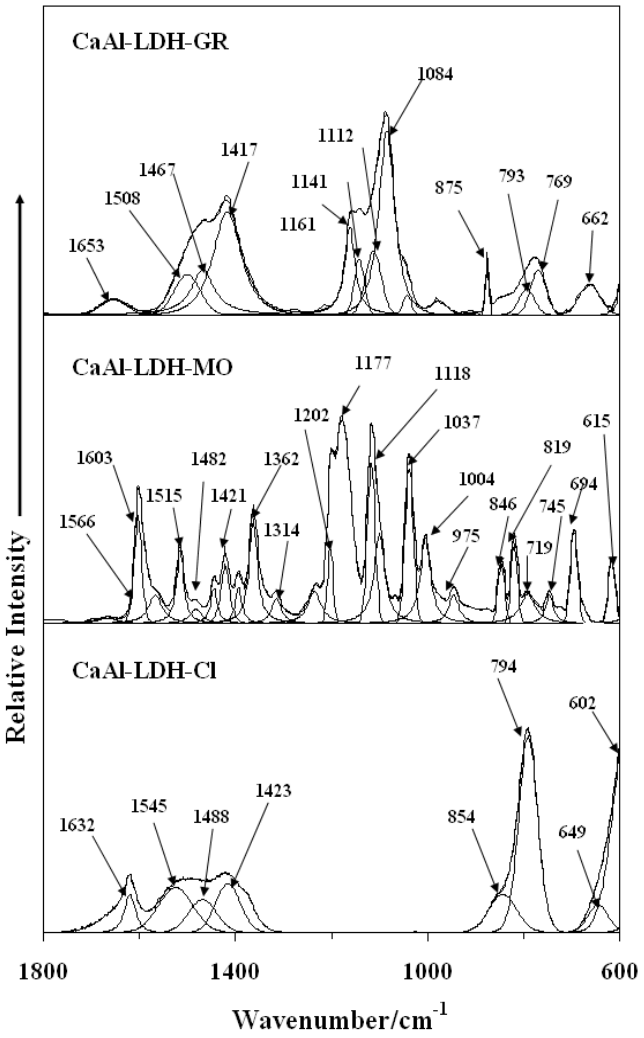

217

218 The mid-infrared spectra in range of 1800-600 cm^{-1} for Ca/Al-LDH-Cl,
219 Ca/Al-LDH-Cl reacted with methyl orange and acidic scarlet GR were
220 present in Fig. 2 and Table. 1. In the infrared spectrum of original
221 Ca/Al-LDH-Cl, the structural bands at 900–600 cm^{-1} were responsible for
222 the stretching vibrations modes of *M*-O, *M*-O-*M*, and O–*M*–O bonds,
223 where M means metal atoms, and O means oxygen atoms. The broad
224 bands around 1632 cm^{-1} were mainly attributed to the bending mode of
225 the structural water. IR spectroscopy was very sensitive to carbonate

226 anions in LDHs (v_{1423} cm^{-1}), with the weak band here it was assumed that
227 the prepared samples contained a small amount of carbonate. Compared
228 with the MIR spectra of Ca/Al-LDH-Cl, in case of the Ca/Al-LDH-MO,
229 the N-H bending vibration emerged at 1515 cm^{-1}, the N=N stretching
230 bands were observed at about 1620 and 1440 cm^{-1} and the significant
231 bands of S=O and $–SO_3^-$ group were observed at 1177 and 1037 cm^{-1},
232 respectively. The C-H aromatic out-of-plane bending vibration (846 cm^{-1}),
233 C-H aromatic in-plane bend (1004 and 1118 cm^{-1}), were in positions
234 similar to the published results [29, 40]. Furthermore, it was seen that
235 there were complex bands in the 900-600 cm^{-1} region, attributed to ring
236 vibrational modes. It was interesting to note that the bands related to the
237 *M*-O lattice vibrations disappeared in 900-600 cm^{-1} range, and probably
238 shifted to lower wavenumbers. This phenomenon was in harmony with
239 other reports referred to intercalated materials into the LDHs interlayer [8,
240 41]. It was also indicated that MO^- ion was successfully intercalated into
241 Ca/Al-LDH-Cl interlayer. However, for the MIR spectra of
242 CaAl-LDH-GR, it was easily seen that the bands were similar to those of
243 Ca/Al-LDH-Cl in the range from 900 to 600 cm^{-1}, indicating that *M*-O
244 lattice vibrations showed a small change. Yet there were still some
245 differences from the MIR spectra of CaAl-LDH-GR. It is noted that the
246 N=N stretching, S=O antisymmetric and C-H aromatic in-plane bending
247 were appeared at 1467 cm^{-1}, 1169 cm^{-1}, 1084 and 1112 cm^{-1}, respectively.

3.2.2. The 4000-2750 cm^{-1} spectral region

Fig.3 The 4000 – 2750 cm^{-1} region of IR spectra of samples of Ca/Al-LDH-Cl , Ca/Al-LDH-MO and Ca/Al-LDH-GR

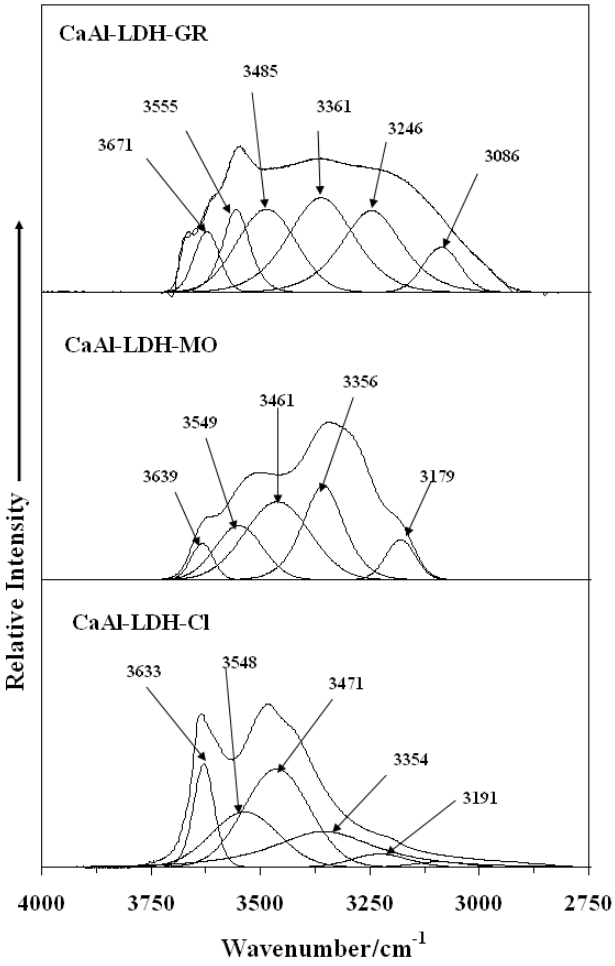

In the infrared spectra between 4000 to 2750 cm^{-1}, the bands of Ca/Al-LDH-Cl were emerged in 3633 and 3548 cm^{-1} attributed to stretching vibrations of interlayer water, and the stretching modes of OH groups appeared at 3471, 3354 and 3191 cm^{-1} [29], respectively (Fig. 3 and Table. 1). In fact, the positions of CaAl-LDH-MO bands were similar

to those of Ca/Al-LDH-Cl (3639, 3461, 3356 and 3179 cm^{-1}), Only with the bands of lattice water becoming shaper (3356 and 3179 cm^{-1}) and the bands of OH stretching getting to broader, indicating the surface property of CaAl-LDH-MO was changed from hydrophilic to hydrophobic [16]. The characteristic band of N-H stretching occurred at 3549 cm^{-1} [16]. Compared to the Ca/Al-LDH-Cl, the bands of OH stretching vibration with CaAl-LDH-GR shifted to higher wavenumbers (3671, 3555 cm^{-1}), and these bands were attributed to interlayer water at 3485, 3361, 3246 and 3086 and shifted to lower wavenumber. In view of two different changes with the stretching vibrations of lattice water and OH groups for CaAl-LDH-MO and CaAl-LDH-GR. It was also proven that methyl orange and acidic scarlet GR had different a different mechanism of interaction with the Ca/Al-LDH-Cl.

3.3. Near-infrared spectroscopy

NIR spectroscopy are the results of energy absorption by organic molecules [42], and often referred to as proton spectroscopy. The NIR technique mainly measures overtones and combination bands of fundamental vibrations of O–H, N–H, and C–H bonds in the mid infrared region [34, 36, 43, 44]. The NIR spectra may be conveniently divided into sections according to the attribution of bands in this spectral region. In terms of methyl orange and acidic scarlet GR both containing O–H, N–H

and C–H bands, their NIR spectra were divided into two sections. They were (a) the spectra region between 5600 and 4000 cm^{-1}, due to combination of OH stretching, N–H stretching and bending modes (Fig. 4 and Table. 2); and (b) the spectral region between 8000-5600 cm^{-1} region corresponded to the second fundamental overtones of OH stretching vibrations (Fig. 5 and Table. 2).

Fig.4 The 5600 – 4000 cm^{-1} region of NIR spectra of samples of Ca/Al-LDH-Cl , Ca/Al-LDH-MO and Ca/Al-LDH-GR

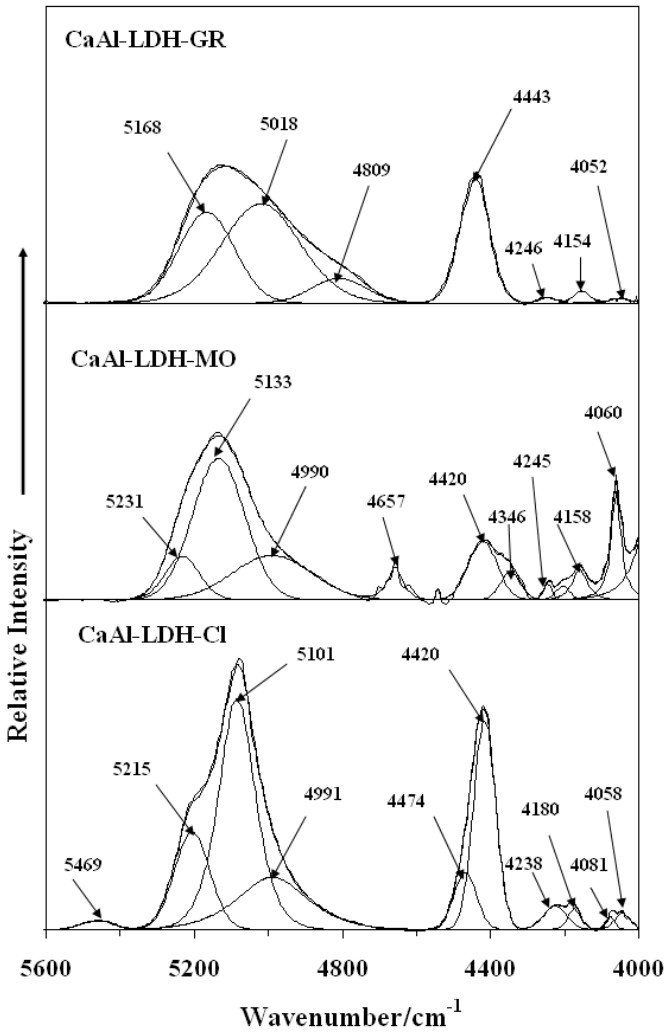

Fig.5 The 8000 – 5600 cm^{-1} region of NIR spectra of samples of Ca/Al-LDH-Cl , Ca/Al-LDH-MO and Ca/Al-LDH-GR

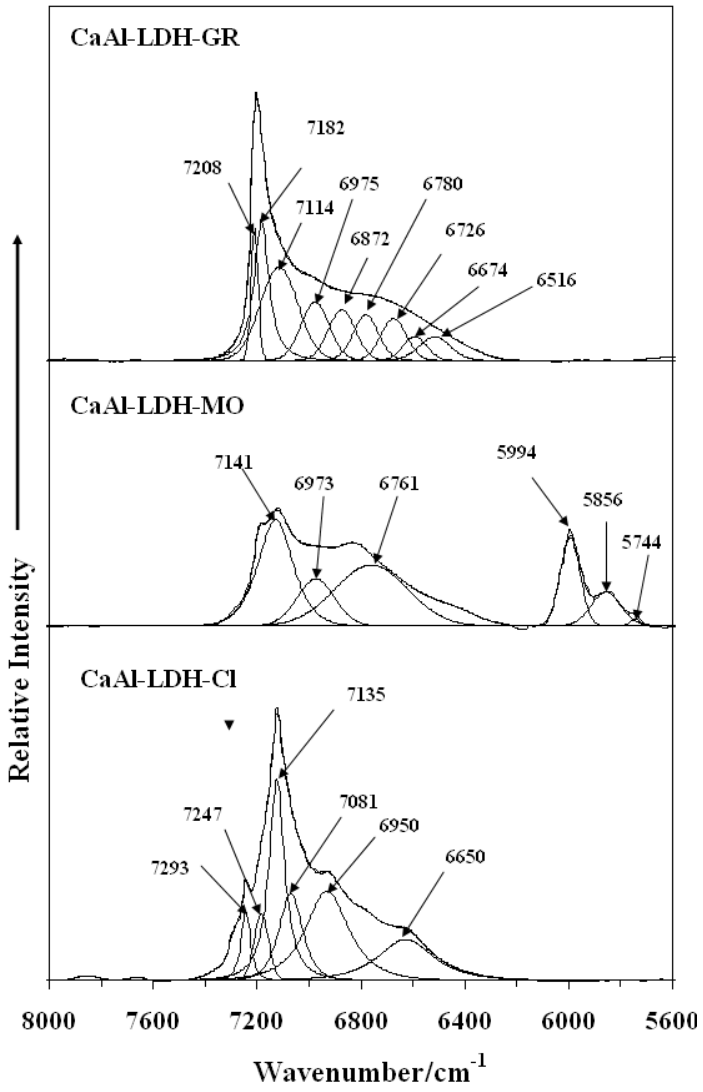

3.3.1 The 5600–4000 cm^{-1} spectral region

The NIR spectra in the range of 5600-4000 cm^{-1} mainly focused on two groups of bands at 5101 and 4420 cm^{-1} for Ca/Al-LDH-Cl and organo-Ca/Al-LDH-Cl with methyl orange or acidic scarlet GR (Fig. 4). The bands of Ca/Al-LDH-Cl centered upon 5101 cm^{-1} were attributed to the

295 overtones of water OH vibrations [44]. The band at 5101 cm^{-1} shifted to
296 5133 cm^{-1} when Ca/Al-LDH-Cl reacted with methyl orange, which was
297 towards the higher wavenumber region, indicating that interlayer surface
298 of Ca/Al-LDH-Cl changed. It was obvious that the overtones of N-H
299 bending vibration at 4657 cm^{-1}. However, for Ca/Al-LDH-GR, these
300 peaks still centered at 5101 cm^{-1}, just became slightly broader. The other
301 groups of bands were shown at 4420, 4238, 4180, 4081 and 4058 cm^{-1}
302 with variable band positions and diminishing intensity corresponding to
303 the overtones and combinations of the vibrational modes of the carbonate
304 ions [45]. This might be due to the combination of the symmetric
305 stretching modes of the $(CO_3)^{2-}$ anion. Thus they were reduced intensity in
306 Ca/Al-LDH-MO, revealing $(CO_3)^{2-}$ anion was replaced by methyl orange
307 ion. In the case of Ca/Al-LDH-GR, the group of relevant bands shifted to
308 4443, 4246, 4154, 4052 cm^{-1}, which all were higher than those of
309 Ca/Al-LDH-Cl. These results were also suggested that methyl orange and
310 acidic occurred two different ways to react with Ca/Al-LDH-Cl, and the
311 former was intercalated into interlayer spacing of Ca/Al-LDH-Cl, while
312 the latter was adsorbed on surface of Ca/Al-LDH-Cl.

313 ***3.3.2 The 8000 – 5600 cm^{-1} spectral region***

314 The NIR spectral region between 8000 and 5600 cm^{-1} was the region
315 where the first fundamental overtone of the OH stretching bands were

316 investigated (Fig. 5). The bands were displayed for Ca/Al-LDH-Cl at
317 7247, 7135, 7081 and 6950 cm^{-1} and attributed to the first fundamental
318 overtone of the OH stretching vibrations in the mid-IR spectrum for
319 Ca/Al-LDH-MO, and the wavenumbers of bands obviously were higher
320 than those of Ca/Al-LDH-Cl, in accordance with the results of MIR.
321 Additionally, the three prominent peaks at 5994, 5856 and 5744 cm^{-1} are
322 assigned to the overtones of the fundamental N-H stretching vibrations.
323 These results provided evidence that MO ion had entered into
324 Ca/Al-LDH-Cl interlayer. Thus, there were similar bands around
325 corresponding positions for Ca/Al-LDH-GR. It was revealed that the
326 structure of Ca/Al-LDH-Cl was not changed after it reacted with acidic
327 scarlet GR. Combined with the XRD results, it was deserved that acidic
328 scarlet GR was attracted to the outside surface and / or the plate edges of
329 Ca/Al-LDH-Cl.

330 ***3.4 SEM***

331 **Fig.6 The SEM images of (a) Ca/Al-LDH-Cl; (b) Ca/Al-LDH-MO**
332 **and (c) Ca/Al-LDH-GR. (The marked spot (in Fig.6b) indicates the**
333 **layered structure of Ca/Al-LDH-Cl)**

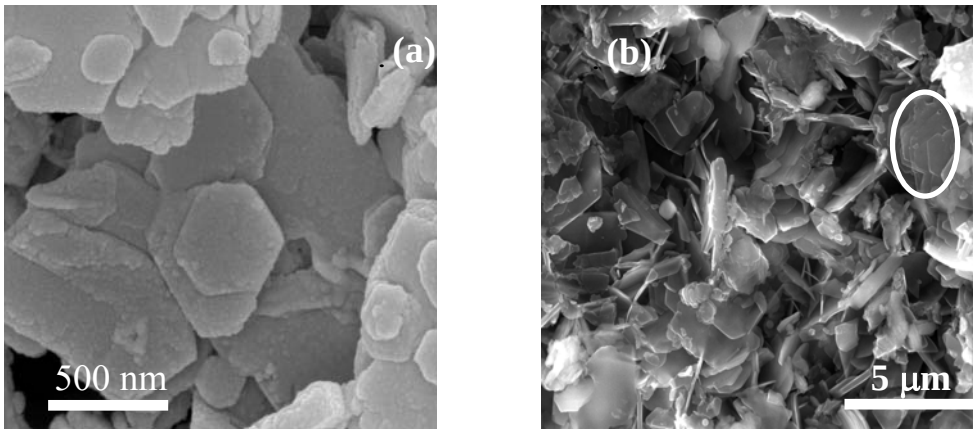

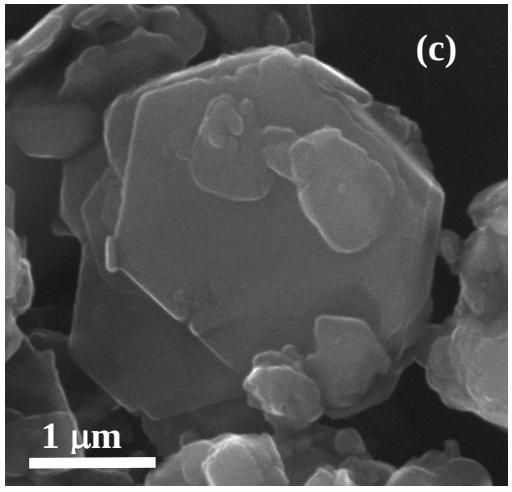

Fig. 6 displays the SEM images of original Ca/Al-LDH-Cl, the Ca/Al-LDH-MO and Ca/Al-LDH-GR. The morphology of Ca/Al-LDH-Cl demonstrated the approximately hexagonal platy crystallites, and it had sharp particle edge and similar particle size. The samples treated with methyl orange and acidic scarlet GR showed different morphology. In the case of Ca/Al-LDH-MO observed in Fig.6b, the particle size became smaller than that of Ca/Al-LDH-Cl. Though the particle plates were still layered structure, the overall morphology

displayed a “honey-comb” like structure, with the distance of adjacent layers expanded. In addition, it was also discovered easily some particles kept the structure of Ca/Al-LDH-Cl (observed as the ring sign marked in Fig.6b), just identical with the XRD results. For the Ca/Al-LDH-GR, it was still kept the layered structure morphology of Ca/Al-LDH-Cl, just some of the particles were agglomerated and interconnected with each other. As observed previously by other authors [46], the surfaces were more diffuse, suggesting that GR was adsorbed over the external surface of Ca/Al-LDH-Cl.

Based on the results discussed above, it is proposed that two different mechanisms of interaction of Ca/Al-LDH-Cl with methyl orange and acidic scarlet GR. The former was an intercalation process, and the latter was an adsorption process. The mechanism of these interaction models are displayed in Fig.7. Generally, high molecular weight organic anions were able to occur intercalation reaction with Ca based LDHs, such as methyl orange anion, polycarboxylate-based anions. They all contained one OSO_3 bond in their structures [47, 48]. Yet the structure of acidic scarlet GR has two OSO_3 bonds (shown as Scheme 1b), they probably prevented acidic scarlet GR anion entering into the interlayer spacing of LDH due to electrostatic repulsion [49], and it occurred adsorption interaction with Ca/Al-LDH-Cl.

Fig.7 The models illustration of methyl orange (MO) and acidic scarlet GR (GR) interacted with Ca/Al-LDH-Cl

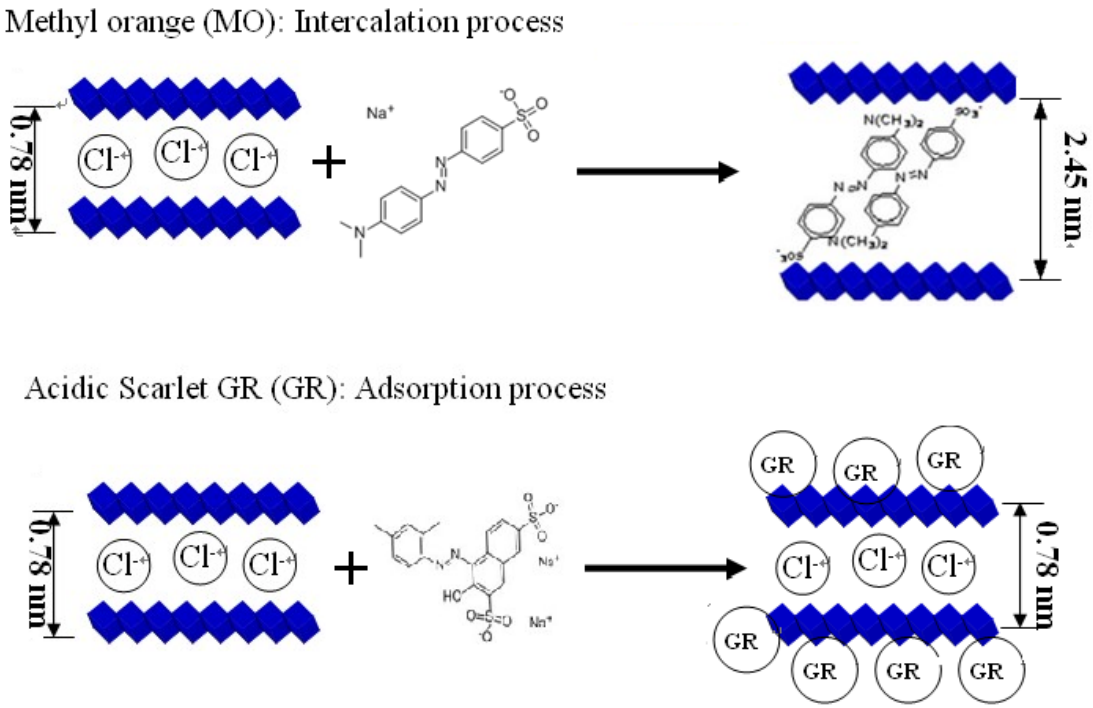

4. Conclusions

In this study, methyl orange and acidic scarlet GR were reacted with Ca/Al-LDH-Cl and formed organo-LDHs. MO^- ion was intercalated into the interlayer spacing of Ca/Al-LDH-Cl, and acidic scarlet GR was simply adsorbed. The changes in the molecular structure of Ca/Al-LDH-Cl were confirmed by the XRD and SEM analysis combining with the MIR and NIR spectroscopic methods. For Ca/Al-LDH-MO, its distance of interlayer spacing was expanded to 2.45 nm, with a inter-penetrating bilayer model, and its tilting angle was calculated as 49^o. The morphology of Ca/Al-LDH-MO remained a layered structure.

Additionally, NIR spectra offered a new and novel method for the proof of the intercalation. The NIR spectroscopy revealed that the spectra from 8000 to 5600 cm^{-1} were more obvious region of N-H bending vibration to determinate methyl orange ion intercalated into Ca/Al-LDH-Cl.

Acknowledgments

The authors gratefully acknowledge infra-structure and morphology checking support of the Queensland University of Technology, Chemistry Discipline, Faculty of Science and Technology. This project is financially supported by National Nature Science Foundation of China No 20907029 and No. 20677037, Shanghai Leading Academic Discipline Project No. S30109.

390 **References**

391 [1] N.N. Das, J. Konar, M.K. Mohanta, S.C. Srivastava, Journal of
392 colloid and interface science 270 (2004) 1.

393 [2] M.O. Adebajo, R.L. Frost, Energy & Fuels 19 (2005) 783.

394 [3] K. Grover, S. Komarneni, H. Katsuki, Water Research 43 (2009)
395 3884.

396 [4] N. Iyi, K. Tamura, H. Yamada, Journal of colloid and interface
397 science 340 (2009) 67.

398 [5] J.-H. Choy, S.-J. Choi, J.-M. Oh, T. Park, Applied Clay Science 36
399 (2007) 122.

400 [6] H. Zhao, K. Nagy, Journal of colloid and interface science 274 (2004)
401 613.

402 [7] J. Pisson, C. Taviot-Gueho, Y. Israeli, F. Leroux, P. Munsch, J. Itie, V.
403 Briois, N. Morel-Desrosiers, J. Besses, J. Phys. Chem. B 107 (2003)
404 9243.

405 [8] F.R. Costa, A. Leuteritz, U. Wagenknecht, D. Jehnichen, L. Häußler,
406 G. Heinrich, Applied Clay Science 38 (2008) 153.

407 [9] A. Legrouri, M. Lakraimi, A. Barroug, A. De Roy, J. Besse, Water

408 Research 39 (2005) 3441.

409 [10] A.K. Suryavanshi, J.D. Scantlebury, S.B. Lyon, Cement and
410 Concrete Research 26 (1996) 717.

411 [11] J. Plank, Z. Dai, N. Zouaoui, Journal of Physics and Chemistry of
412 Solids 69 (2008) 1048.

413 [12] U. Birnin-Yauri, F. Glasser, Cement and Concrete Research 28
414 (1998) 1713.

415 [13] P. Zhang, H. Shi, R. Xiuxiu, Q. Guangren, R. Frost, J. Therm.
416 Anal. Calorim. (2010) 1.

417 [14] Y. Dai, G. Qian, Y. Cao, Y. Chi, Y. Xu, J. Zhou, Q. Liu, Z.P. Xu, S.
418 Qiao, Journal of Hazardous Materials 170 (2009) 1086.

419 [15] Y. Wu, Y. Chi, H. Bai, G. Qian, Y. Cao, J. Zhou, Y. Xu, Q. Liu, Z.P.
420 Xu, S. Qiao, Journal of Hazardous Materials 176 (2010) 193.

421 [16] J. Wang, X. Ren, X. Feng, S. Liu, D. Sun, Journal of Colloid and
422 Interface Science 318 (2008) 337.

423 [17] Z.-M. Ni, S.-J. Xia, L.-G. Wang, F.-F. Xing, G.-X. Pan, Journal of
424 Colloid and Interface Science 316 (2007) 284.

425 [18] E. Haque, J.W. Jun, S.H. Jhung, Journal of Hazardous Materials

426 185 (2011) 507.

427 [19] A. Demirbas, Journal of Hazardous Materials 167 (2009) 1.

428 [20] G. Crini, Bioresource Technology 97 (2006) 1061.

429 [21] A.I. Gupta VK, Saini VK., J. Colloid Interface Sci 315 (2009) 7.

430 [22] I. Ali, V.K. Gupta, Nat. Protocols 1 (2007) 2661.

431 [23] D.B.N. Bharat N. Patila, and V.S. Shrivastavaa, J. Colloid
432 Interface Sci 309 (2007) 6.

433 [24] Environ. Sci. Technol 42 (2008).

434 [25] V.K. Gupta, P.J.M. Carrott, M.M.L. Ribeiro Carrott, Suhas,
435 Critical Reviews in Environmental Science and Technology 39 (2009)
436 783.

437 [26] V.K. Gupta, A. Mittal, V. Gajbe, J. Mittal, Journal of Colloid and
438 Interface Science 319 (2008) 30.

439 [27] A.M. Vinod K. Guptaa, Rajeev Jainc, Megha Mathurc,Shalini
440 Sikarwarc, J. Colloid Interface Sci 303 (2006) 7.

441 [28] R.J. Vinod Kumar Guptaa, Shaily Varshneyb,Vipin Kumar Sainia,
442 J. Colloid Interface Sci 307 (2007) 7.

443 [29] L.-Y. Liu, M. Pu, L. Yang, D.-Q. Li, D.G. Evans, J. He, Materials
444 Chemistry and Physics 106 (2007) 422.

445 [30] R. Marangoni, M. Bouhent, C. Taviot-Guého, F. Wypych, F.
446 Leroux, Journal of Colloid and Interface Science 333 (2009) 120.

447 [31] L.D.R. In, New York: Chapman & Hall (1999).

448 [32] E. Géraud, M. Bouhent, Z. Derriche, F. Leroux, V. Prévot, C.
449 Forano, Journal of Physics and Chemistry of Solids 68 818.

450 [33] H. Chung, M.-S. Ku, J.-S. Lee, Vibrational Spectroscopy 20 (1999)
451 155.

452 [34] H. Cheng, Q. Liu, J. Yang, J. Zhang, R.L. Frost, X. Du, Journal of
453 Molecular Structure 990 (2011) 21.

454 [35] J. Madejová, M. Pentrák, H. Pálková, P. Komadel, Vib Spectrosc
455 49 (2009) 211.

456 [36] R. Liu, R.L. Frost, W.N. Martens, Materials Chemistry and
457 Physics 113 (2009) 707.

458 [37] L. Lu, J. Cai, R.L. Frost, Spectrochim Acta A: Mol Biomol
459 Spectrosc 75 (2010) 960.

460 [38] M. Bouraada, F. Belhalfaoui, M.S. Ouali, L.-C. de Ménorval,

461 Journal of Hazardous Materials 163 (2009) 463.

462 [39] M.-X. Zhu, Y.-P. Li, M. Xie, H.-Z. Xin, Journal of Hazardous
463 Materials 120 (2005) 163.

464 [40] L. El Gaini, M. Lakraimi, E. Sebbar, A. Meghea, M. Bakasse,
465 Journal of Hazardous Materials 161 (2009) 627.

466 [41] C. Liu, W. Hou, L. Li, Y. Li, S. Liu, Journal of Solid State
467 Chemistry 181 (2008) 1792.

468 [42] E.W.C. D.A. Burns, Marcel Dekker. Inc. New York (1992) 7.

469 [43] R.L. Frost, H.J. Spratt, S.J. Palmer, Spectrochimica Acta Part A:
470 Molecular and Biomolecular Spectroscopy 72 (2009) 984.

471 [44] H. Cheng, J. Yang, Q. Liu, J. Zhang, R.L. Frost, Spectrochimica
472 Acta Part A: Molecular and Biomolecular Spectroscopy 77 (2010) 856.

473 [45] R.L. Frost, S. Bahfenne, J. Graham, B.J. Reddy, Polyhedron 27
474 (2008) 2069.

475 [46]

476 [47] B. Yu, H. Bian, J. Plank, Journal of Physics and Chemistry of
477 Solids 71 (2010) 468.

478 [48] J. Plank, D. Zhimin, H. Keller, F.v. Hössle, W. Seidl, Cement and

480 [49] X. Wang, N. Zhu, B. Yin, Journal of Hazardous Materials 153
481 (2008) 22.

482

483

484 Table 1 Summary of MIR wavenumbers and their assignment for
485 CaAl-LDH-Cl , CaAl-LDH-MO and CaAl-LDH-GR (cm^{-1})

CaAl-LDH-Cl	CaAl-LDH-MO	CaAl-LDH-GR	Assignment
3633, 3548,	3356 and 3179	3485, 3361, 3246 ,3086	stretching vibrations of lattice water
3471, 3354 and 3191	3639, 3461,	3671, 3555	The stretching vibration of the OH groups
	3549		N-H stretching vibration
1632			the bending mode of the interlayer structural water
	1620, 1440	1467	the N=N

			stretching
		1169	S=O antisymmetric
	1515		the N-H bending vibration
	1177, 1037		S=O and $–SO_3^-$ group
	1004, 1118	1084 , 1112	C-H aromatic in-plane bend
	975, 819	875, 793, 769, 662	ring vibration
854, 794, 649, 602			the *M*-O lattice vibrations
	846		The C-H aromatic out-of-plane bending vibration

491

492

493

494

495

496 Table 2 Summary of NIR wavenumbers and their assignment for
497 CaAl-LDH-Cl , CaAl-LDH-MO and CaAl-LDH-GR (cm^{-1}).

CaAl-LDH-Cl	CaAl-LDH-MO	CaAl-LDH-GR	Assignment
7247□7135□ 7081□6950	7141, 6973 , 6761	7208, 7182, 7114, 6975, 6872, 6726,6674, 6516	The first fundamental overtone of the OH stretching vibrations
	5994, 5856 and 5744		the overtone of N-H stretching vibration
5101	5231, 5133, 4990		the overtones of water OH vibrations
	4657		the overtones of N-H bending vibration
4420, 4238, 4180,		4443, 4246, 4154,	the combination

4081 and 4058		4052	of the symmetric stretching modes of the $(CO_3)^{2-}$ anion

498

499

500

501 **List of Tables**

502 Table 1 Summary of MIR wavenumbers and their assignment for
503 CaAl-LDH-Cl , CaAl-LDH-MO and CaAl-LDH-GR (cm^{-1})

504 Table 2 Summary of NIR wavenumbers and their assignment for
505 CaAl-LDH-Cl , CaAl-LDH-MO and CaAl-LDH-GR (cm^{-1})

506 **List of Scheme1**

507 **List of Figures**

508 Fig.1 XRD patterns of samples of Ca/Al-LDH-Cl, Ca/Al-LDH-MO and
509 Ca/Al-LDH-GR scanned from 5°-65° (a) and 1°-15° (b)

510 Fig.2 The 1800 - 600 cm^{-1} region of IR spectra of samples of
511 Ca/Al-LDH-Cl , Ca/Al-LDH-MO and Ca/Al-LDH-GR

512 Fig.3 The 4000 – 2750 cm^{-1} region of IR spectra of samples of
513 Ca/Al-LDH-Cl , Ca/Al-LDH-MO and Ca/Al-LDH-GR

514 Fig.4 The 5600 – 4000 cm^{-1} region of NIR spectra of samples of
515 Ca/Al-LDH-Cl , Ca/Al-LDH-MO and Ca/Al-LDH-GR

516 Fig.5 The 8000 – 5600 cm^{-1} region of NIR spectra of samples of
517 Ca/Al-LDH-Cl , Ca/Al-LDH-MO and Ca/Al-LDH-GR

518 Fig.6 The SEM images of (a) Ca/Al-LDH-Cl; (b) Ca/Al-LDH-MO and (c)
519 Ca/Al-LDH-GR. (The marked spot (in Fig.6b) indicates the layered
520 structure of Ca/Al-LDH-Cl; The marked spot (in Fig.6c) indicates
521 adsorption position of acidic scarlet GR)

522 Fig.7 The models illustration of methyl orange and acidic scarlet GR
523 interacted with Ca/Al-LDH-Cl

524

525 **Scheme 1**

526

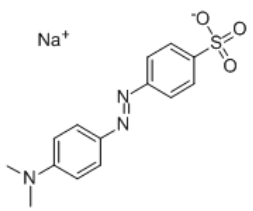

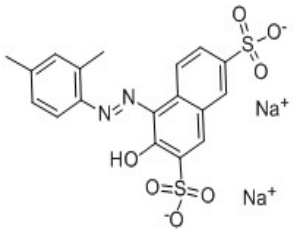

527 **Methyl orange** **Acidic scarlet GR**

528 Fig.1 XRD patterns of samples of Ca/Al-LDH-Cl, Ca/Al-LDH-MO and

529 Ca/Al-LDH-GR scanned from 5°-65° (a) and 1°-15° (b)

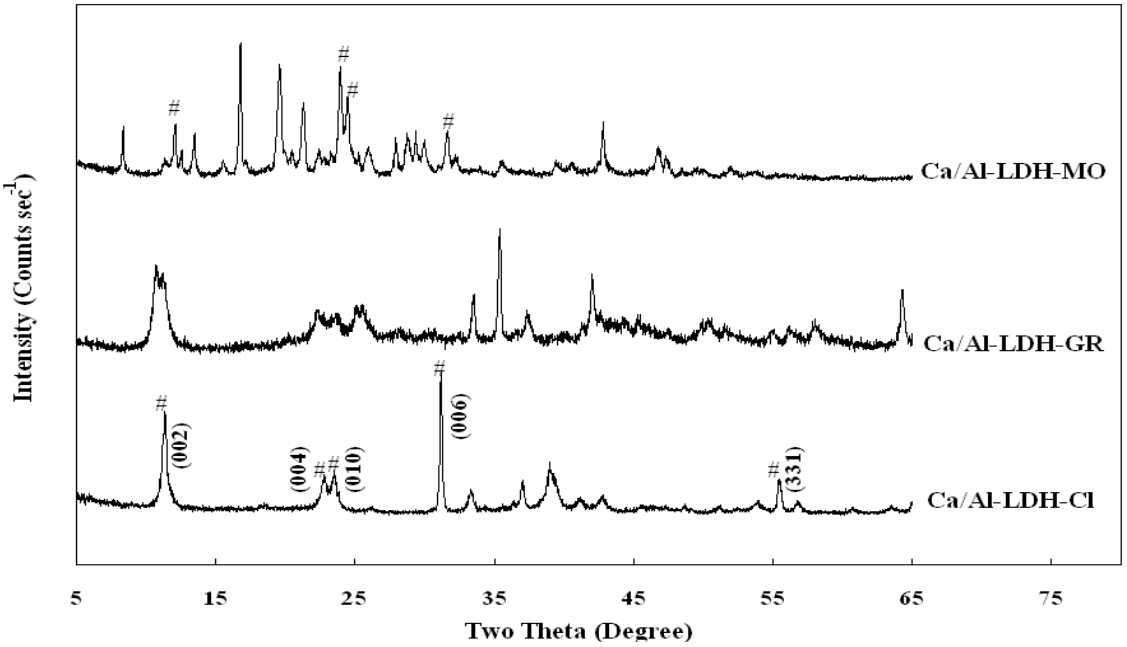

530

531 (a)

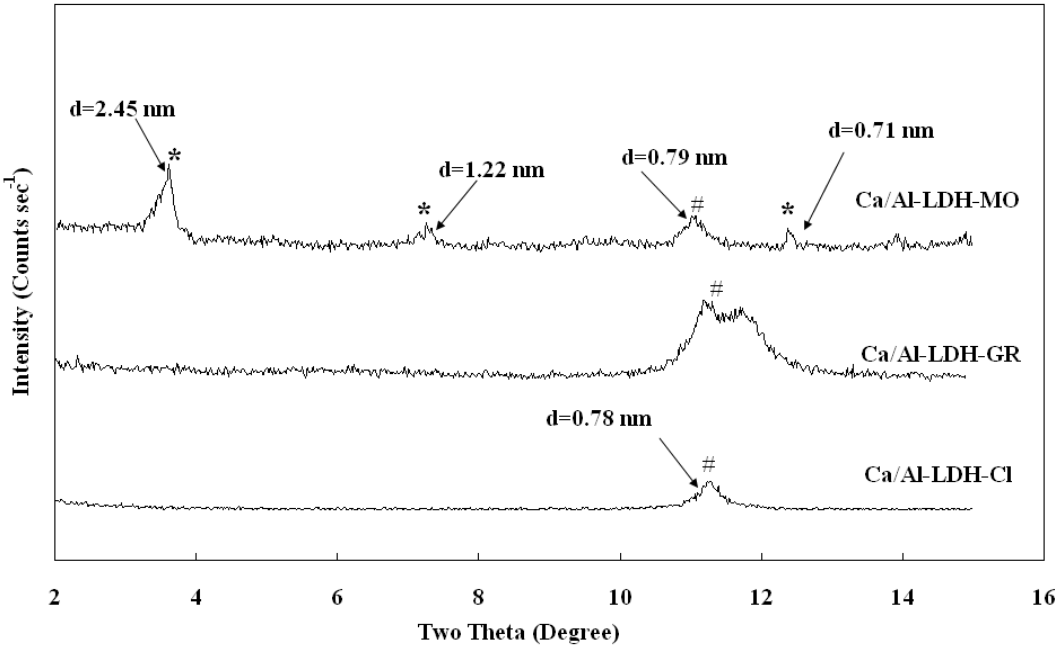

532

533 (b)

534 Fig.2 The 1800 - 600 cm^{-1} region of IR spectra of samples of

535 Ca/Al-LDH-Cl , Ca/Al-LDH-MO and Ca/Al-LDH-GR

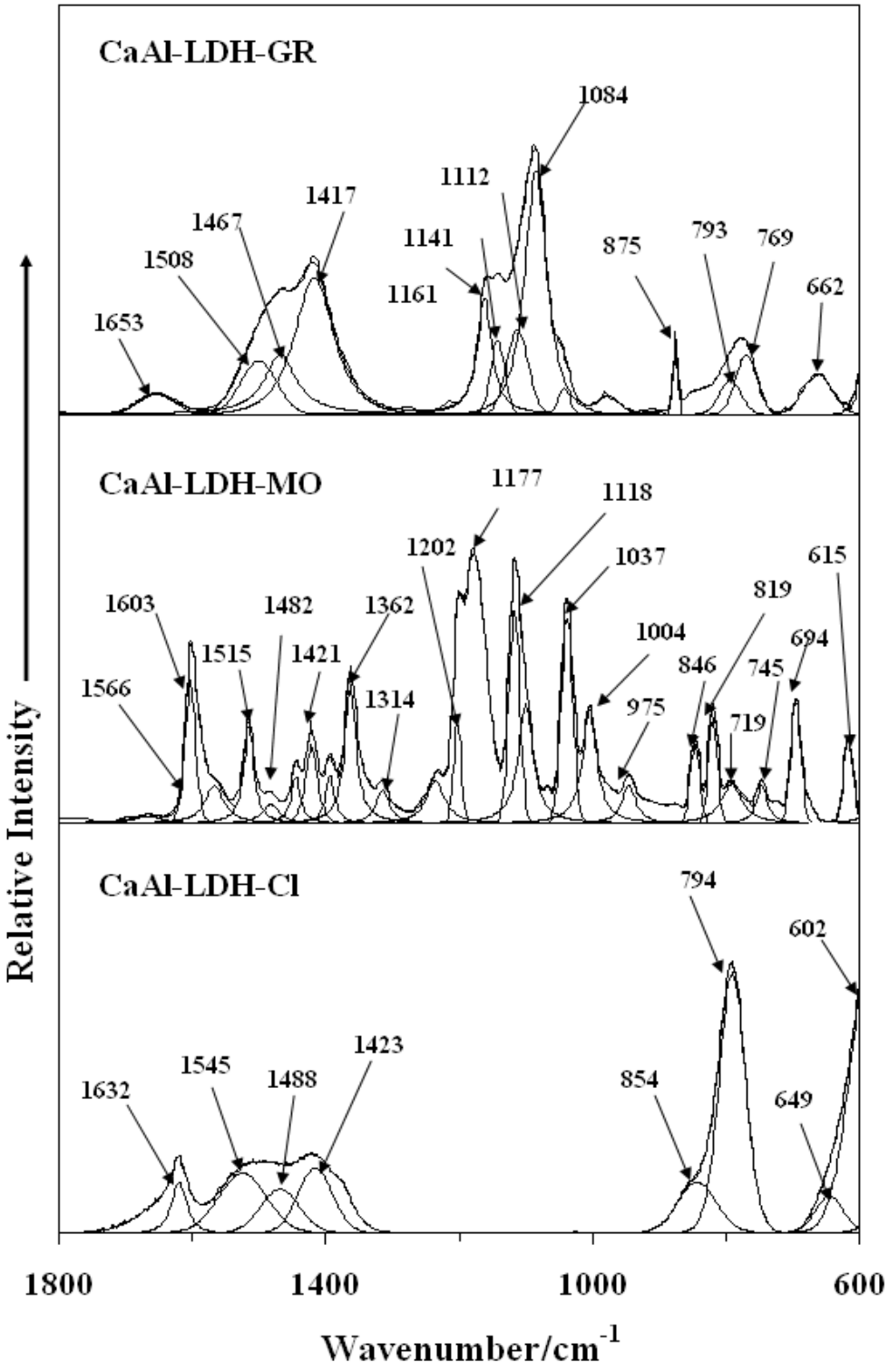

536

537 Fig.3 The 4000 – 2750 cm^{-1} region of IR spectra of samples of

538 Ca/Al-LDH-Cl , Ca/Al-LDH-MO and Ca/Al-LDH-GR

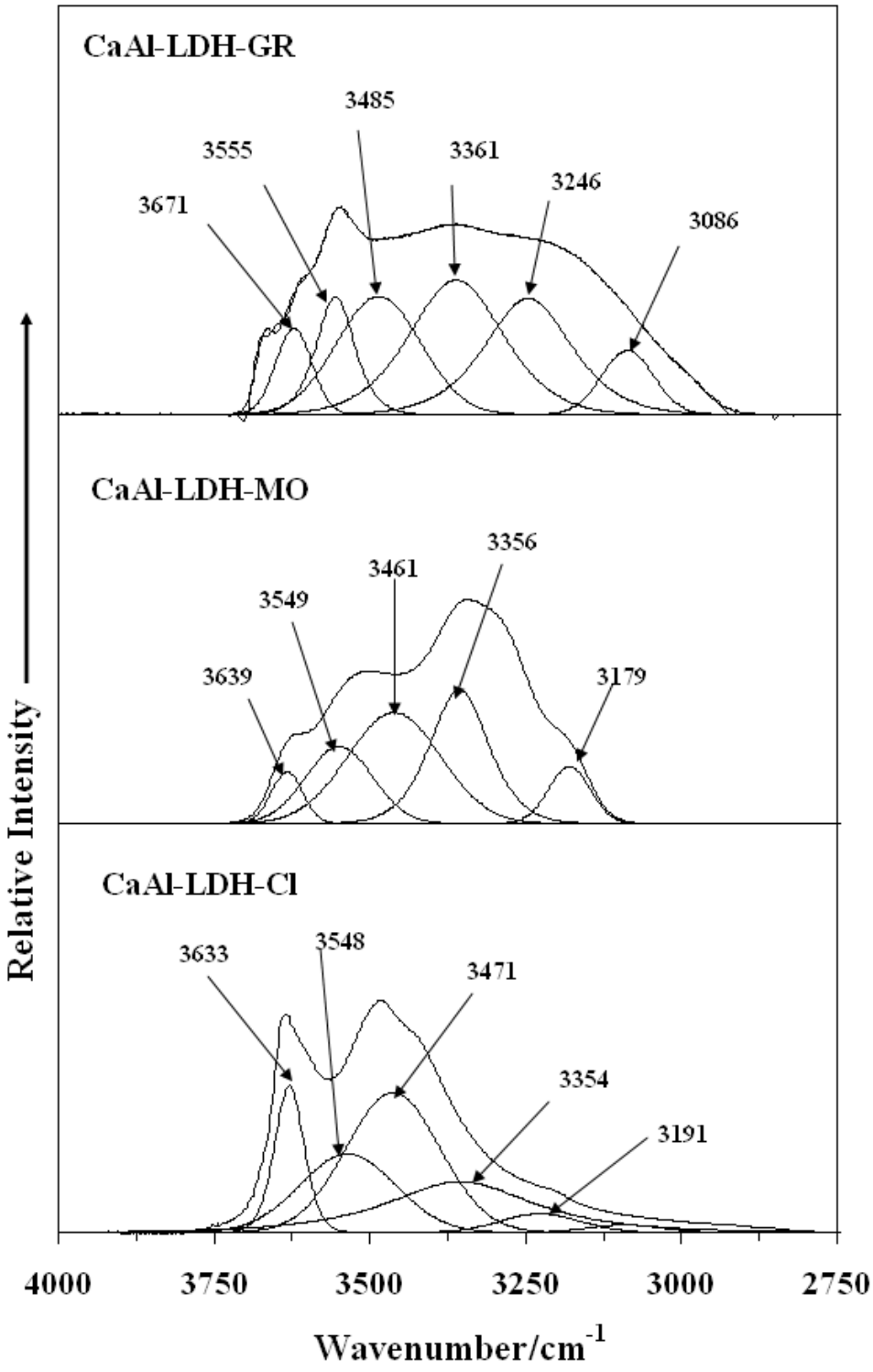

539

Fig.4 The 5600 – 4000 cm^{-1} region of NIR spectra of samples of Ca/Al-LDH-Cl , Ca/Al-LDH-MO and Ca/Al-LDH-GR

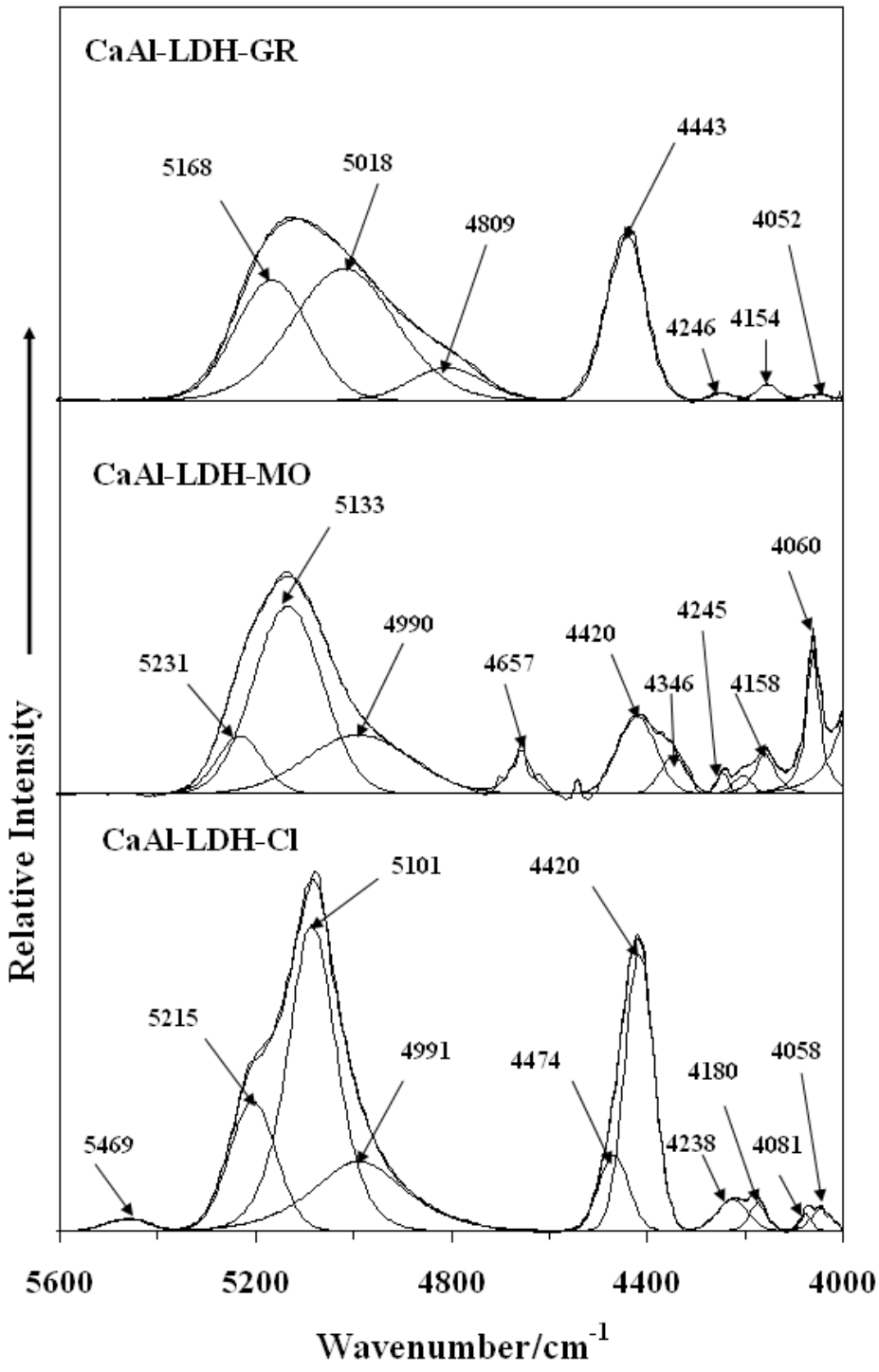

544 Fig.5 The 8000 – 5600 cm^{-1} region of NIR spectra of samples of

545 Ca/Al-LDH-Cl , Ca/Al-LDH-MO and Ca/Al-LDH-GR

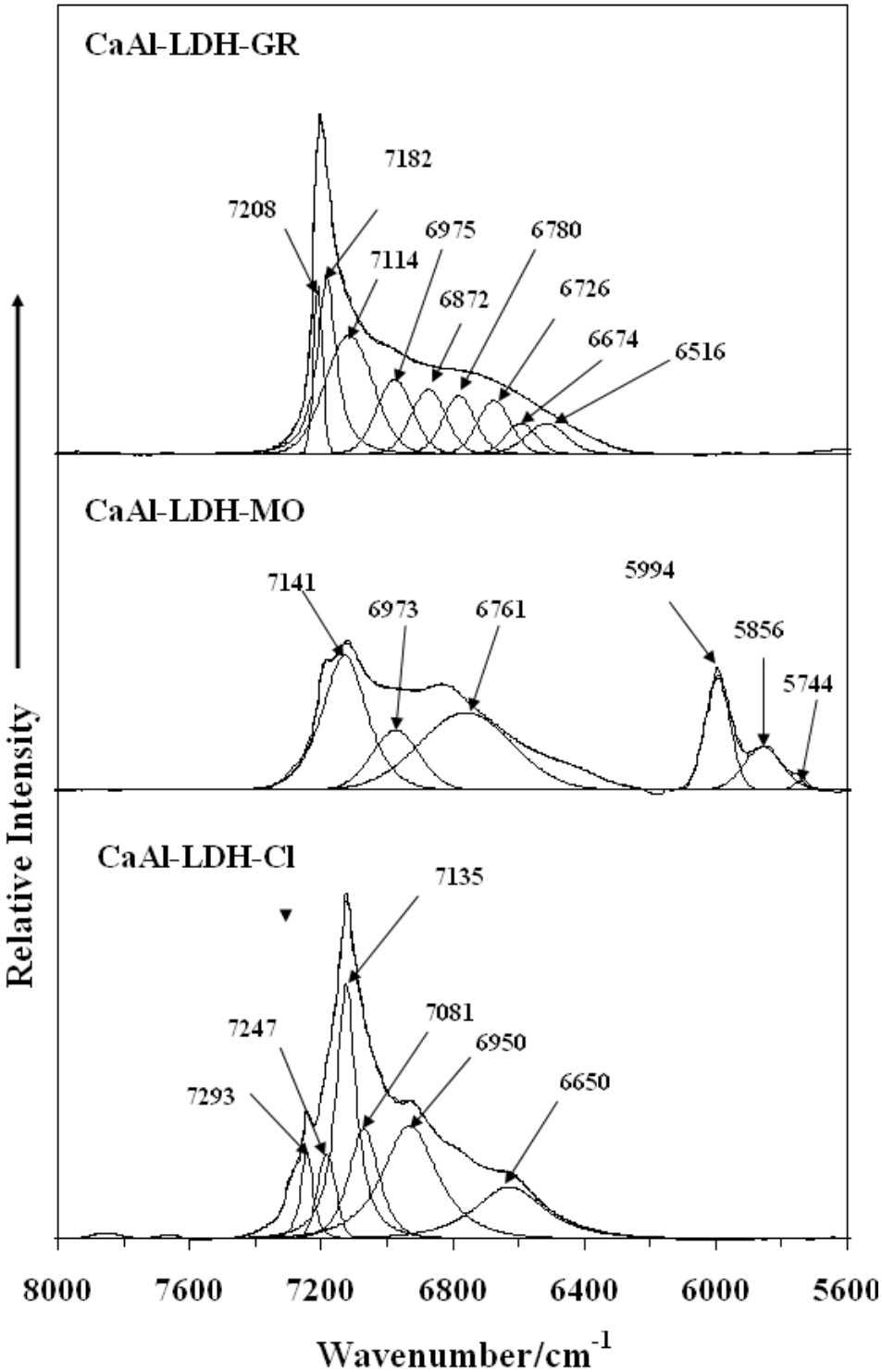

546

547

548 Fig.6 The SEM images of (a) Ca/Al-LDH-Cl; (b) Ca/Al-LDH-MO and (c)
549 Ca/Al-LDH-GR. (The marked spot (in Fig.6b) indicates the layered
550 structure of Ca/Al-LDH-Cl)

551 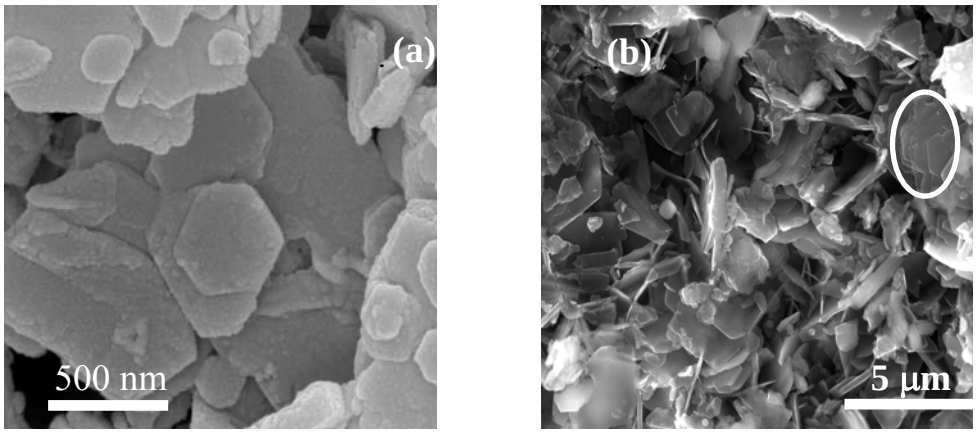

552

553 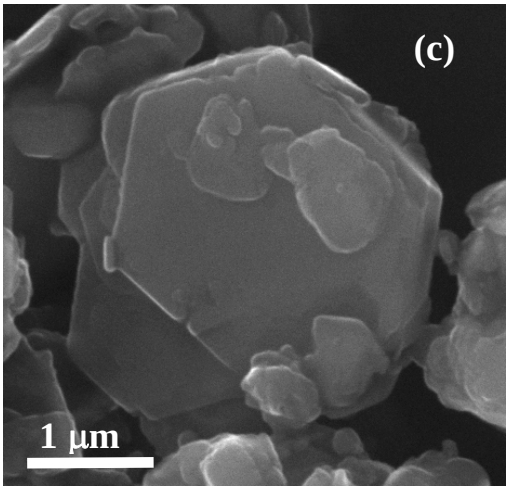

554

555

556 Fig.7 The models illustration of methyl orange (MO) and acidic scarlet
557 GR (GR) interacted with Ca/Al-LDH-Cl

Methyl orange (MO): Intercalation process

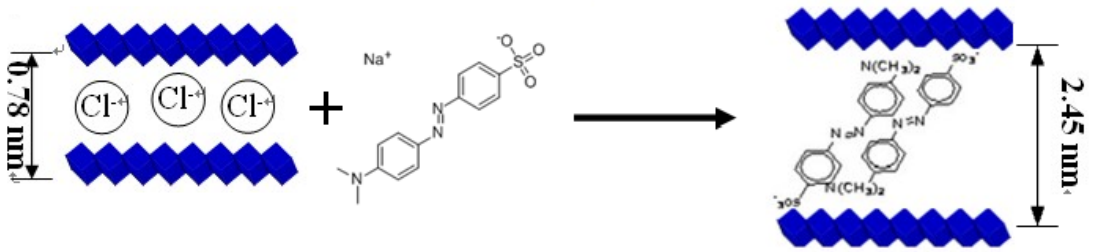

Acidic Scarlet GR (GR): Adsorption process

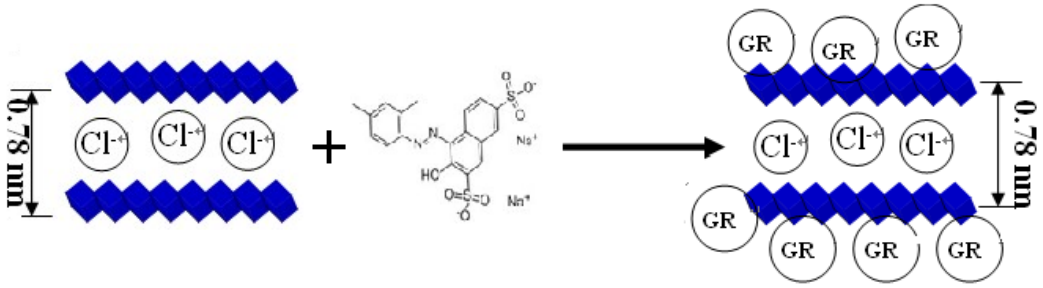

558

559

560

561

562

563

564

(Adsorption process)